Cellular Physiology and Biochemistry

Cell Physiol Biochem 2019;53:532-549
DOI: 10.33594/000000156
Published online: 13 September 2019
Accepted: 5 September 2019

Original Paper

Assessment of Silver-Nanoparticles-Induced Erythrocyte Cytotoxicity through Ion Transport Studies

Norma C. Adragna[a] Praveen K. Alla[a] Ioana E. Pavel-Sizmore[b] Arathi S.L. Paluri[b] Jerome Yaklic[c] Peter K. Lauf[a,d]

[a]Department of Pharmacology and Toxicology, Boonshoft School of Medicine, Wright State University, Dayton, OH, USA, [b]Department of Chemistry, College of Science and Mathematics, Wright State University, Dayton, OH, USA, [c]Department of Obstetrics and Gynecology, Boonshoft School of Medicine, Wright State University, Dayton, OH, USA [d]Department of Pathology, Boonshoft School of Medicine, Wright State University, Dayton, OH, USA

Key Words
Silver nanoparticles • Human adult and cord red blood cells • K^+ and Rb^+ transport • Nanoparticles functionalization • Hyperspectral imaging

Abstract
Background/Aims: Silver nanoparticles (AgNPs) are the most frequently used nanomaterials in industrial and biomedical applications. Their functionalization significantly impacts their properties and potential applications. Despite the need to produce, investigate and apply them, not much is known about the toxicity of silver nanoparticles to and their interaction with blood components, such as erythrocytes. Here, we report on the effect of two negatively charged AgNPs (Creighton, and Lee-Meisel) on ion transport in human red blood cells (HRBCs). ***Methods:*** HRBCs were obtained from blood of adult donors, which was either expired, fresh or refrigerated for variable lengths of time, and from fresh or refrigerated cord blood. Rb^+ and K^+ ions were measured by atomic emission and absorption spectrophotometry, respectively. Erythrocyte hemoglobin optical density (Hb_c OD), was determined at 527 nm to estimate RBC volume in the same tubes in which Rb^+ and K^+ were measured. Cellular Rb^+ uptake and intracellular K^+ concentrations, $[K]_i$, were calculated in mmol/L of original cells (LOC) per time. Rubidium, a potassium ion (K^+) congener used to measure K^+ influx, $[K]_i$, and Hb_c ODs were determined in the presence and absence of several concentrations (0-150 μg mL^{-1}) of spherical AgNPs of an average diameter of 10 nm, at different time points (0-60 min). ***Results:*** Creighton AgNPs inhibited Rb^+ influx and depleted the cells of K^+ independently of the source and in a time and dose-dependent manner. In contrast, Lee-Meisel AgNPs caused ~ 50 % Rb^+ influx inhibition and ~ 15 % K^+ loss with larger interindividual variability than Creighton AgNPs. The loss of K^+ from HRBCs was entirely accounted for by an increase in extracellular K^+ concentration, $[K]_o$. Enhanced dark field optical microscopy in conjunction with CytoViva®

Norma C. Adragna, Ph.D. Department of Pharmacology & Toxicology, Wright State University, Boonshoft School of Medicine Dayton, OH 45435 (USA)
Tel. +1 937-775-2889, E-Mail norma.adragna@wright.edu

hyperspectral imaging helped visualize AgNPs internalized by HRBCs, thus pointing to a potential cause for their cytotoxic effects. ***Conclusion:*** These findings indicate that HRBC K^+ homeostasis is an early and sensitive biomarker for AgNPs toxicity and is a function of their surface functionalization.

Introduction

Numerous studies have concentrated on the groundbreaking discoveries and applications of Nanotechnology, summarized by Roco et al. in a recent report [1] and further demonstrated by more recent findings [2, 3]. Silver nanoparticles (AgNPs) are the most frequently used nanomaterials for applications in Nanotechnology and Nanomedicine. The large surface area and high reactivity of AgNPs, in addition to their shape, are responsible for their bactericidal properties [4-6], which became of great interest in the early 2000s when multidrug-resistant bacteria were causing significant number of casualties in the human population [7-9]. This trend has continued developing with more promising results [2, 10-14]. In addition to the therapeutic properties of AgNPs, it became apparent that they also possess toxic effects in a large variety of systems, such as in mammalian germline stem cells [15], mammalian cells [16], spermatogonial stem cells [17], burn wounds [18], alveolar macrophages [19], human hepatoma cells [20], human lung cancer cells [21, 22], cultured keratinocytes [23], fibroblasts [24], and, in general, at the organismal, cellular and sub-cellular levels [2, 21, 22, 25-31]. Small nano-size particles are more likely to be internalized into cell lines than their large counterparts [32, 33]. Different types of NPs are known to induce cytotoxicity in various cell lines and animal models. AgNPs are extremely toxic because of their metallic silver and its high biological reactivity [34, 35]. Chronic exposure of keratinocytes to low doses of AgNPs to mimic more realistic exposure showed striking differences to acute studies [36]. In humans, colloidal nano silver has been shown to cause *Argyria* (a grayish discoloration of the skin [37].

AgNPs cause red blood cells (RBCs) deformation, agglutination and membrane damage [38]. AgNPs elicit RBCs hemolysis due to their large surface area, which facilitates an increased release of silver ion (Ag^+) by direct interaction with RBCs [32, 39]. In fact, released Ag^+ appears to be responsible for the AgNPs toxicity [40-42]. In human RBCs, AgNPs change the conformation of oxyhemoglobin to its deoxy form, which may be the result of a decrease in intracellular pH induced by the NPs [43]. In fish RBCs, decreasing the size of AgNPs from 100 to 15 nm increases their toxicity [44], although some studies have shown that the toxicity of Ag^+ vs. AgNPs is dependent on their ratio [21]. In contrast, biogenic AgNPs possess bactericidal effects without eliciting the commonly known toxic effects of the non-biogenic [45]. Positively charged NPs are more toxic than the negatively charged [46] because the surface charge on RBCs is negative and thus possess higher affinity for the positively charged NPs. In human RBCs, internalized quantum dots (QDs) by D-penicillamine (DPA-QDs), enter the cells by a passive transport mechanism, and their toxicity is due to the cationic QDs [32].

However, few studies providing a detailed mechanism of AgNPs toxicity are available despite their abundant applications in industry and in AgNPs-based medicine, where they have been introduced into human tissue mostly upon administration by either injection or through skin exposure. These penetration routes will likely lead to interaction of AgNPs with blood tissue and its components [47, 48] and can be either beneficial or detrimental. For instance, AgNPs synergistically activate immune responses by human blood monocytes [49]. In contrast, AgNPs cause structural damage of erythrocytes and change erythrocyte rheology [38]. AgNPs also cause platelet aggregation and hemolysis of RBCs [50, 51].

Assessment of AgNPs toxic effects thus becomes a key task science must address given the fact that the predicted environmental concentrations already exceed the predicted no-effect AgNPs concentrations [52]. Furthermore, and in contrast to the abundance of information on AgNPs beneficial and toxic effects, relatively few studies have been reported on their effect on cellular function [53], and particularly on ion transport mechanisms in

human RBCs [54, 55]. The importance of using blood and its components to assess both beneficial and toxic effects of AgNPs, and of nanomaterials in general, stems from the fact that once the NPs reach the circulating blood, one of the major tissues of the body with a plasma/erythrocyte ratio close to unity, they are the most likely compartments to become in contact with the NPs. Although white cells and platelets represent a significantly smaller blood compartment, NPs effects on them are certainly not negligible [51]. Most importantly, alterations of membrane permeability and ion transport are one of the early events leading to cell death, thus becoming a strategic point for applying maneuvers to reverse the NPs toxic effects.

The present study reports on the effect of two widely-used, negatively charged AgNPs on K^+ transport metabolism in human adult and cord RBCs.

Materials and Methods

Chemicals

Tris-hydroxyamino methane (Tris) free base, sodium chloride (NaCl), magnesium chloride ($MgCl_2$), sodium phosphate ($NaPO_4$), sodium hydroxide (NaOH), and D-glucose were acquired from Fisher Scientific (Fair Lawn, NJ). The compound 3-morpholinopropane-1-sulfonic acid (MOPS) was from Sigma-Aldrich (St. Louis, MO); rubidium chloride (RbCl), 99.8 % (metals basis), from Alfa Aesar (Ward Hill, MA); cesium chloride (CsCl), from Life Technologies (Carlsbad, CA) and Acationox detergent from Baxter (Oxford labware (Illinois).

Silver Nanoparticles (AgNPs)

AgNPs were synthesized by the Creighton (CR) method [53, 56-58] and the Lee- Meisel (LM) method [59]. CR AgNPs were synthesized in an ice bath by the dropwise titration reduction of silver nitrate (50 mL of 1 mM $AgNO_3$) with sodium borohydride (300 mL of 2 mM $NaBH_4$). LM AgNPs were obtained under heating at about 90°C by the reduction of silver nitrate (1.7 mL of 1% $AgNO_3$) with trisodium citrate (2 mL of 1% $Na_3C_6H_5O_7$) in 100 mL of water. Both reaction mixtures were stirred (~320 rpm) for 1 hour to ensure completion. The original colloid of CR AgNPs was size-selected, purified and concentrated by tangential flow filtration (TFF) (KrosFlo Research IIi)) using 500 kD (790 cm^2, ~50 nm pore size) and 10 kD (790 cm^2, ~5 nm pore size) modified polyether sulfone (mPES) filters and the retentate was collected [53, 56, 60-62]. For LM AgNPs, the colloid was concentrated by centrifugation and then filtered through a 10 kD filter to remove any free Ag^+ present in the colloid (< 10 %) [53, 62]. Thus, the Ag^+ core of CR AgNPs was protected by borate and the LM AgNPs by citrate ions. Both AgNPs were suspended in deionized water. Except for the capping agent, the average size (10 nm), shape (spherical) and color (deep brown) of CR and LM AgNPs were the same [53, 62].

Blood

Concentrated red blood cells (RBCs) were donated by the Dayton Community Blood Center (DCBC), and human cord and adult blood by the Miami Valley Hospital (MVH), Dayton, OH. Packed RBCs from the DCBC were collected with citrate, phosphate, and dextrose (CPD) as anticoagulant and suspended in a preservation solution, mostly Optisol (AS-5, see below), to prolong storage [63, 64]. An additive solution was used to store RBCs up to 42 days at 2-6 °C, which contained adenine besides mannitol and NaCl, each at different concentrations, (AS) AS-1, AS-3 and AS-5 (http://www.mahasbtc.com/preservation-and-storage-blood). Cord blood (CB) was collected after C-sections at MVH and was a mixture of arterial and venous blood. The blood was collected into K^+ ethylene diamine tetra-acetic acid (K_2EDTA) vacutainer tubes and stored at 4° C until further use.

Ion transport determination

Whole blood (WB) obtained from MVH was collected in Vacutainer tubes and was used to determine the hematocrit (Hct) and optical density (OD) of packed cells (ODpcs). The ODpcs was obtained by diluting an aliquot of WB in hemolyzing solution (HS) (201X). ODs were measured in a Gilford Spectrophotometer (Gilford Systems, Oberlin, OH) at 527 nm, *i.e.*, the isosbestic point for oxy- and met-hemoglobin (Hb) spectra

[65]. The OD_{pcs} for concentrated RBCs were calculated as described for cord blood. WB or concentrated RBCs were centrifuged at 10,000 rpm for 5 min to separate the RBCs from plasma and buffy coat that were aspirated and discarded. The packed RBCs remaining were collected and used for further studies.

For ion transport determination, several experimental solutions were required. Initial washing solution, composed of NaCl, 300 mOsM at room temperature (RT). Preincubation solution made of K^+-free phosphate-buffered saline (PBS) containing (mM): 5 $NaPO_4$ buffer, 5 Glucose, and NaCl to adjust osmolality to 295 mOsM, pH 7.4 at RT. Flux solutions containing (mM): 5 $NaPO_4$ buffer, 10 RbCl, 5 Glucose, NaCl, pH 7.4, to adjust osmolality to 295 mOsM. Final washing solution containing (mM): 10 MOPS/Tris-$MgCl_2$, pH 7.4, 4 °C, 295 mOsM. Hemolyzing solution containing (mM): 4 CsCl, 29 % NH_4OH, and Acationox detergent.

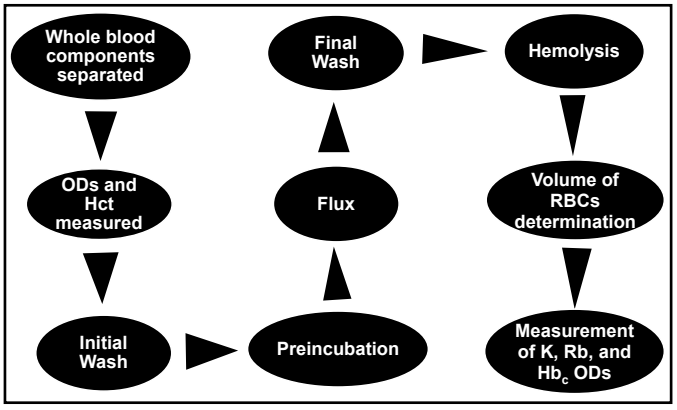

Fig. 1. Schematic diagram of the steps involved in the preparation of human red blood cells (HRBCs) for the determination of Rb influx, intracellular K concentration $[K]_i$ and cellular hemoglobin (Hb_c) optical densities (ODs).

Experimental Procedure

The RBC pellet obtained after WB or concentrated RBCs centrifugation was washed 4X with the initial washing solution at 37 °C, and spun until the centrifuge reached 10,000 rpm, at which point, centrifugation was stopped. The initial wash with isosmotic NaCl solution maintained the original cellular volume and served to remove anticoagulants and other chemicals. Then, RBCs were pre-incubated in PBS for 15 min at 37 °C, centrifuged in a Sorval RC5 ultracentrifuge at 10,000 rpm up and down, and the supernatant discarded. This step was also used to equilibrate RBCs with different chemicals, as needed, prior to exposure to the flux solutions. The technique for ion fluxes determination was adapted from previously published work [66] with some modifications for the NPs study as indicated next. RBCs were incubated at 37 °C in flux media as described above, and in the absence or presence of AgNPs for 1 h, swirling every 15 min. After 1 h of incubation, triplicates were prepared and washed 3X in final washing solution and spun down using an Eppendorf centrifuge (Eppendorf North America, Hauppauge, NY) at 14,000 rpm (18,188 g). Rb^+ and K^+ ions were extracted from RBCs with hemolyzing solution and measured by atomic emission and absorption spectrophotometry, respectively, using a Perkin Elmer 5000 atomic absorption spectrophotometer (Perkin Elmer Corporation, Waltham, MA). Hb_c OD, was determined at 527 nm to estimate RBC volume in the same tubes in which Rb^+ and K^+ were measured. Cellular Rb^+ uptake and $[K]_i$ were calculated in mmol/L of original cells (LOC) per time. Fig. 1 summarizes the steps described in this section.

Statement of Ethics

Concentrated red blood cells (RBCs) were donated by the Dayton Community Blood Center (DCBC), and human cord blood by the Miami Valley Hospital (MVH), Dayton, OH. Subjects (or their parents or guardians) have given their written informed consent and the study protocol was approved by the institute's committee on human research under IRB # 06216, SC # 6034. Part of this work has been previously presented at the Experimental Biology Annual Meetings and published as abstracts in FASEB J. 2016, and 2017, and as a master's thesis by one of the co-authors (P.K.A.).

Results

Two types of spherical AgNPs, average diameter of 5-10 nm with a narrow size distribution (1-40 nm) after filtration, and negatively charged ($AgNPs^-$) were successfully

synthesized by the CR and LM methods and used in this study [53, 62], see Materials and Methods for further details).

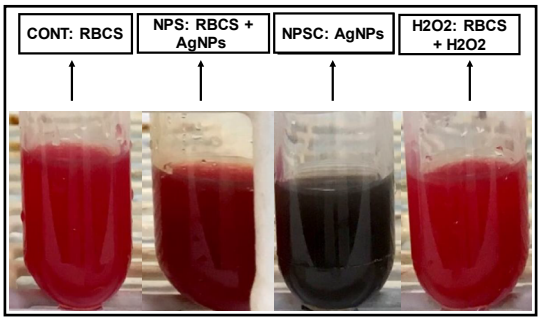

Fig. 2. Effect of negatively charged Creighton (CR) AgNPs ($AgNPs^-$) and oxidation on coloration of HRBCs. Tube 1: Flux media + RBCs (CONT); Tube 2: AgNPs + flux media + RBCs (NPS); Tube 3: Flux media + NPS (NPSC); Tube 4: Hydrogen peroxide in flux media + RBCs (H_2O_2).

Studies with Creighton (CR) AgNPs

Washed human cord red blood cells (RBCs) were incubated with CR $AgNPs^-$, for 1 h at 37 °C (Fig. 2) under the following conditions: 1 = CONT, RBCs incubated in the absence of $AgNPs^-$ in a medium of the same osmolality as NPS; 2 = NPS, RBCs + medium + $AgNPs^-$; 3 = NPSC, a $AgNPs^-$ control to take into account AgNPs potential interference in both cation and RBC volume determinations; 4 = Hydrogen peroxide (H_2O_2), a known oxidant and positive control in flux media + RBCs. The sample containing AgNPs showed a visible color change suggesting oxidation of RBC Hb_c to $MetHb_c$ [67], which was spectrophotometrically confirmed by a decrease in absorbance of 10-15 % for peak A (Mean ± Range, 537.5 ± 1.5 nm, n = 2) and 10-30 % for peak B (Mean ± Range, 574.5 +/- 2.5 nm, n = 2) when compared to the CONT. The Hb_c spectrum also showed an additional broad shoulder between 594.1 and 658.8 nm probably due to MetHb formation (Results not shown).

Effect of CR AgNPs on Rb^+ influx, $[K]_i$ and Hb_c ODs in adult RBCs

Next, the effect of AgNPs on Rb^+ influx and $[K]_i$ of human RBCs was studied in a pilot experiment (data not shown) on two day-expired RBCs from the DCBC. CR AgNPs completely inhibited Rb^+ influx and depleted $[K]_i$ ($p < 0.0001$, n = 7, and $p < 0.001$, n = 7, respectively). This unexpected finding was thought to be due to the expired RBCs, which may have been leaky and prone to hemolysis. Alternatively, since AgNPs cause hemolysis of RBCs [51, 68], inhibition of Rb^+ influx and the almost complete K^+_i loss was thought to be due to hemolysis. Contrary to this expectation, determination of Hb_c ODs, a measure of the relative volume of RBCs for each condition, showed a significant difference in ODs between CONT and NPS ($p < 0.0001$, n = 12) indicating that the RBC volume in the latter was about 2-fold higher than that in CONT and almost at the level of the isotonic control (CONTC, see Fig. 3 below) dispelling doubts about RBC hemolysis as a cause of the results observed in expired RBCs and affirming that the observed $[K]_i$ depletion was indeed an effect caused by the AgNPs.

Thus, in Fig. 3 the entire experimental regimen of the pilot experiment with expired blood was repeated by studying the effect of CR AgNPs on Rb^+ influx (Fig. 3A), $[K]_i$ (Fig. 3B) and Hb_c ODs (Fig. 3C) in fresh human adult blood. Three of the four conditions chosen are those previously described for Fig. 2, CONT, NPS and NPSC. An additional control was added in Fig. 3, CONTC = isotonic control of normal osmolality. As explained in Fig. 2, the control NPSC is required to correct for other confounding factors, such as light scattering or absorbance of AgNPs near the wavelength of Hb_c ODs determinations.

Exposure of fresh RBCs to $AgNPs^-$ at a concentration of 150 μg mL^{-1} inhibited ~ 100 % of Rb^+ influx and caused a total $[K]_i$ loss (Fig. 3A and B, respectively) ($p < 0.0001$ vs. the control, n = 12). There was a statistically significant difference in Hb_c ODs between CONT and NPS ($p < 0.0001$, n = 12) (Fig. 3C). The decrease in Hb_c ODs in cells exposed to AgNPs appears to be in part due to cell swelling thus lowering the OD_s with the hypoosmotic AgNPs suspension, and to some hemolysis. Furthermore, despite a lower Hb_c ODs in AgNPs-exposed RBCs, the values are within those observed for expired adult RBCs, indicating presence of RBCs in all conditions tested. A statistically significant difference between CONTC and CONT ($p < 0.001$, n = 12) was also observed, which may be due to osmolality differences between these two media (Fig. 3C).

It was not clear from the transport data whether NPs that were adsorbed to the RBC surface through an electrostatic effect could attract the main intracellular cation, K^+, and thus cause its depletion. In addition, in this case, the inhibition of Rb^+ influx could have occurred by also binding of the extracellular cation to the adsorbed AgNPs. Another possibility is that AgNPs exerted their effect by penetrating the RBCs. This alternative is supported by studies on internalization of quantum dots (QD) as D-penicillamine (DPA)-QD in human RBCs [40].

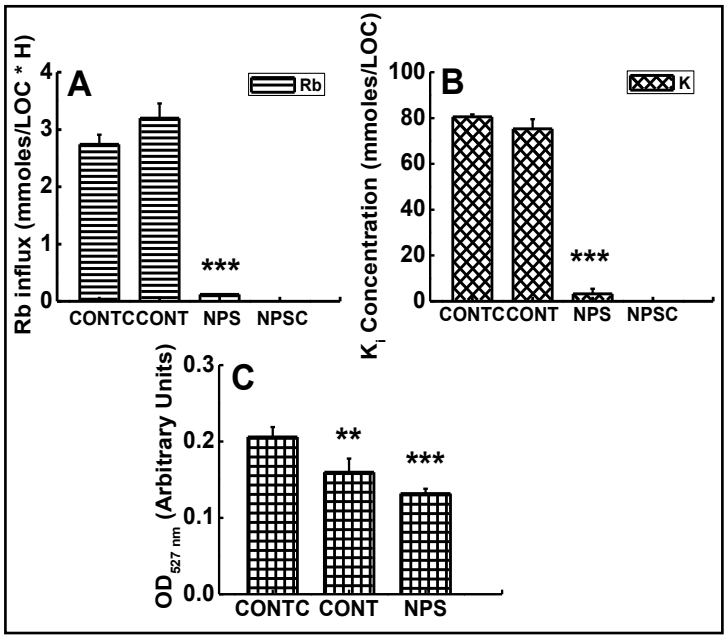

Fig. 3. Effect of CR AgNPs$^-$ on Rb^+ influx, $[K]_i$, and Hb_c ODs in RBCs from adult human blood. A, B and C, Rb^+ influx, $[K]_i$, and Hb_c ODs, respectively, in RBCs from adult human donors donated by the Dayton Community Blood Bank (DCBC) were subjected to the procedures described in Materials and Methods and shown in Fig. 1. During the flux period, RBCs were incubated at 37 °C for 60 min under the following conditions: CONTC (RBCs + flux media), CONT (RBCs + flux media + H_2O), NPS (RBC+ flux media+ AgNPs), and NPSC (AgNPs + flux media). Rb^+ influx, $[K]_i$ and Hb_c ODs were determined as described in Materials and Methods. Values are mean ± S.D for a representative experiment, n = 6 individual determinations for all the conditions tested. The statistical significance of the differences between NPS vs CONT, and CONT vs CONTC for Rb^+ influx and $[K]_i$ concentration (*** $p<0.0001$, n = 6) was determined by two sample t- test. For ODs, the statistical significance of the difference between NPS vs CONT (*** $p<0.0001$, n = 6) and CONT vs CONTC (** $p<0.001$, n = 6) was also determined by two sample t- test. Further details are discussed in the text.

The above question was answered by hyperspectral imaging with a CytoViva® instrument. Fig. 4A-D shows the CytoViva® optical image of a control RBC, an RBC exposed to CR AgNPs$^-$, the hyperspectral image of the RBC exposed to the AgNPs$^-$ revealing the presence of the NPs taken up by the RBCs, and the hyperspectral signatures of AgNPs (green spectrum) and RBCs (red spectrum), respectively. For further details, see legend to Fig. 4. Thus, the unexpected effects observed in RBCs exposed to AgNPs$^-$ were indeed caused by their penetration into the cytosol instead of the sole adsorption onto the RBC surface. Therefore, the inhibition of Rb^+ influx and complete loss of K^+_i may be due to other mechanisms caused by the AgNPs themselves.

Effect of CR AgNPs on Rb^+ influx, $[K]_i$, and Hb_c ODs in cord RBCs

To rule out that results shown in the previous figures were a property of "adult" blood samples, i.e., due to "aging", the effect of CR AgNPs$^-$ on Rb^+ influx and $[K]_i$ was studied in human cord blood (Fig. 5). After incubation of cord RBCs with CR AgNPs for 60 min at 37 °C, Rb^+ influx was completely inhibited ($p < 0.0001$, n = 6). In addition, Rb^+ influx in CONT was higher than in CONTC ($p < 0.005$, n = 6) (Fig. 5A), probably due to a lower osmolality in the CONT, or to differences between cord and adult RBCs, or to interindividual variability within a given blood type, adult expired or fresh, and cord blood. Exposure of cord RBCs to CR AgNPs led to K^+ depletion when compared to their control (CONT) ($p < 0.00001$, n = 6, Fig. 5B), and statistically significant difference was also found in $[K]_i$ between CONT and CONTC (p

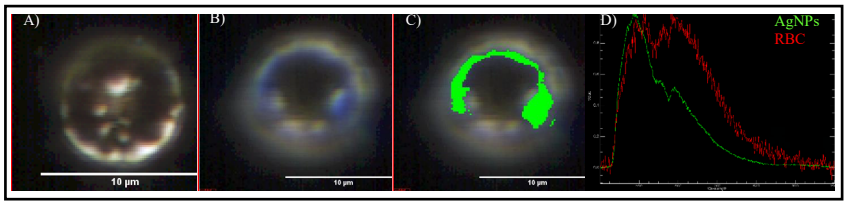

Fig. 4. Hyperspectral imaging of CR AgNPs in human red blood cells. CytoViva® optical image of A) a control red blood cell (RBC), B) a RBC exposed to negatively charged CR AgNPs of 10 nm in diameter for 1 h, and C) the same RBC exposed to AgNPs- after mapping the AgNPs spectral library created at B) against the hyperspectral image. The "green" color coded pixels reveal the presence of $AgNPs^-$, which were taken up by the RBC. D) Hyperspectral signatures of AgNPs (green spectrum) and RBC (red spectrum) controls used in the component's identification. CytoViva® System Description: The images and data were captured using an Olympus research grade optical microscope equipped with CytoViva (Auburn, AL) patented enhanced darkfield illumination optics and full spectrum aluminum halogen source illumination. The CytoViva® system was used in conjunction with a hyperspectral imaging system, producing spectral image files from 400-1,000 nm at 2 nm spectral resolution. CytoViva's customized version of ENVI hyperspectral image analysis software was utilized to quantify the spectral response of the sample and to conduct any spectral mapping of the sample elements.

< 0.005, n = 6, Fig. 5B). Hb_c ODs were about 2-fold higher in NPS with respect to its control (CONT, p < 0.00001, n = 6) (Fig. 5C), and closer to the level of CONTC. The borderline statistical difference in Hb_c ODs between CONT and CONTC (p < 0.061, n = 6) could be due to some hemolysis induced by osmolality differences between these conditions. Inhibition of Rb^+ influx and K^+ depletion from RBCs (Fig. 5A & B) suggest a direct effect of the AgNPs on K^+ metabolism in cord RBCs and independent of the donor's age.

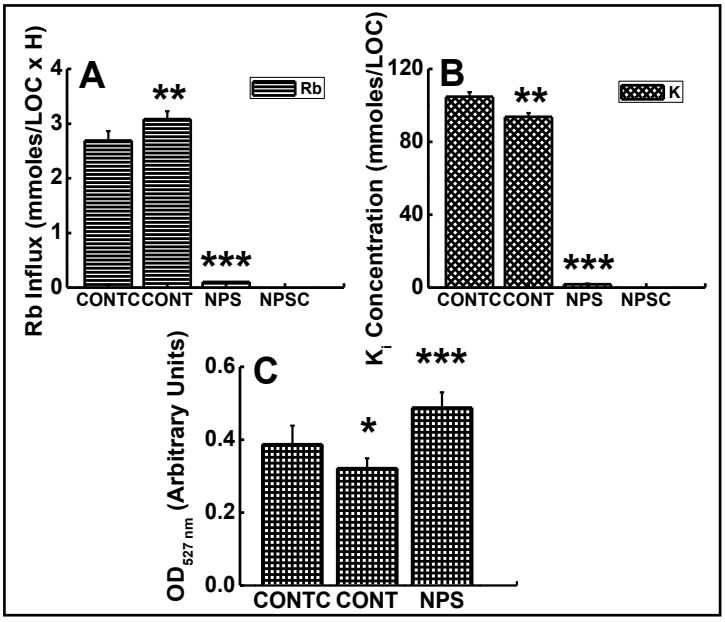

Fig. 5. Effect of CR $AgNPs^-$ on Rb^+ influx, $[K]_i$, and Hb_c ODs in RBCs from human cord blood. Cord blood donated by MVH was subjected to the procedures described in Materials and Methods and Fig. 1. During the flux period, cells were incubated at 37 °C for 60 min under the conditions described in legend to Fig. 3. A) Rb^+ influx, B) $[K]_i$ and C) ODs at 527 nm for Rb^+ influx and $[K]_i$ were determined as described in Materials and Methods. Values are mean ± S.D. for a representative experiment, n = 6 individual determinations for all the conditions tested. The statistical significance of the differences between NPS vs CONT, and CONT vs CONTC was determined by two sample t- test. Further details are discussed in the text. A) *** p<0.00001, ** p<0.005, B) *** p<0.00001, ** p<0.005, and C) ***p<0.00001, * p = 0.061.

Time course of Rb^+ influx, $[K]_i$, and Hb_c ODs as a function of CR AgNPs-exposure in cord RBCs

Some reports on human RBCs indicate that AgNPs induce lysis and structural damage [38, 44, 50]. An indication that the effect of AgNPs on Rb^+ influx and $[K]_i$ is due to the NPs and not to other factors was obtained from kinetic studies such as time-course and dose-dependence. Thus time-course studies were done under the conditions described for Fig. 3.

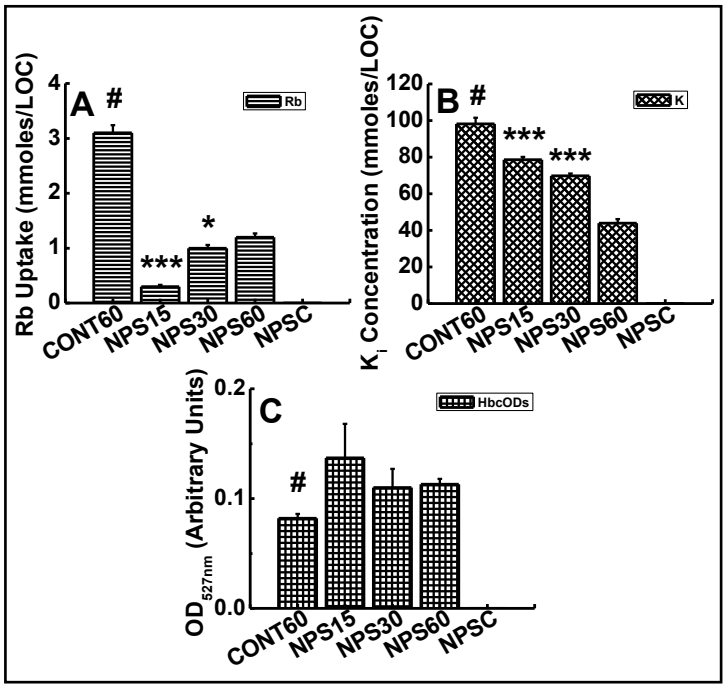

Fig. 6. Time course of Rb^+ uptake, $[K]_i$, and Hb_c ODs in CR AgNPs-treated RBCs from human cord blood. Cord blood donated by MVH was subjected to the procedures described in Materials and Methods and Fig. 1. During the flux period, cells were incubated at 37°C for 15, 30, and 60 min under the conditions described in legend to Fig. 3. A) Rb^+ uptake, B) $[K]_i$ and C) Hb_c ODs at 527 nm for Rb^+ uptake and $[K]_i$. Values are mean ± S.D. for a representative experiment, n= 6 individual determinations for all the conditions tested. The statistical significance of the differences between NPS60 vs NPS15 or NPS30 and NPS60 vs CONT60 was determined by paired t- test. Further details are discussed in the text. A) *** and # p = 0.0000 for NPS15 vs NPS60 and NPS60 vs CONT60, respectively; * p<0.05 for NPS30 vs NPS60. B) *** and # p = 0.0000 for NPS15 vs NPS60, NPS30 vs NPS60, and NPS60 vs CONT60, respectively; and C) # p = 0.0001 forNPS60 and CONT60.

Rb^+ uptake in CR AgNPs-exposed cord RBCs (NPS), increased by ~ 4-fold from 15 to 60 min incubation (Fig. 6A, p = 0.0000, n = 6 for NPS15 vs. NPS60 and p < 0.05 between NPS30 vs NPS60), whereas $[K]_i$ decreased by 2-fold in the same time period (Fig. 6B, p = 0.0000, n =6 for NPS15 or NPS30 vs NPS60). In addition, both Rb^+ influx and $[K]_i$ were about 3-fold lower in NPS than in the CONT at 60 min (Fig. 6A and B, p < 0.0000, n = 6, respectively). In contrast, there was no statistically significant change in the Hb_c ODs between 15, 30 and 60 min and the values were higher than the CONT at 60 min (Fig. 6C, p = 0.0001 for NPS60 vs CONT60) suggesting swelling in the absence but not in the presence of AgNPs. However, in contrast to former findings in expired or fresh adult or cord RBCs, where K^+ loss was in the order of 100 % at 60 min exposure, in this patient's RBCs, the $[K]_i$ decreased only by 60 % showing interindividual variability in the response of RBC K^+ transport to AgNPs exposure.

Once the effect of CR AgNPs on Rb^+ influx and $[K]_i$ was demonstrated to be time-dependent, it was important to determine whether their effect was also dose-dependent.

Dose-response of Rb^+ influx, $[K]_i$, and Hb_c ODs as a function of CR AgNPs-exposure in cord RBCs

Fig. 7 shows a dose-response curve for Rb^+ influx, $[K]_i$ and Hb_c ODs as a function of CR AgNPs concentrations (30 – 150 μg mL^{-1}) for CONT and NPS in cord RBCs. Rb^+ influx was measured after incubation with CR AgNPs for 60 min at 37°C. RBCs exposure to the NPs induced more than 2-fold inhibition of Rb^+ influx along the concentration range tested (p < 0.0001, n = 3, Fig. 7A). Moreover, the lowest concentration of 30 μg mL^{-1} already produced a full effect at which Rb^+ influx was inhibited by more than 80 %. An additional 10 % inhibition in Rb^+ influx was noticed at 150 μg mL^{-1}, the highest concentration tested.

Like for Rb^+ influx, cord RBC $[K]_i$ was measured in both CONT and NPS, the latter after incubation with increasing concentrations of CR AgNPs (30 – 150 μg mL^{-1}) for 60 min at 37°C (Fig. 7B). Results show a concentration dependent effect of AgNPs on $[K]_i$ with about 30% inhibition at 30 μg mL^{-1} and depletion of RBC K^+ at the highest concentration tested (150 μg mL^{-1}), ($p < 0.0001$, n = 3, Fig. 7B). Thus, CR AgNPs induce a dose-dependent depletion of $[K]_i$ in cord RBCs, while $[K]_i$ decreased almost linearly by 70%. Furthermore, the kinetics of inhibition was different for Rb^+ and K^+, despite a dose response effect for the two cations.

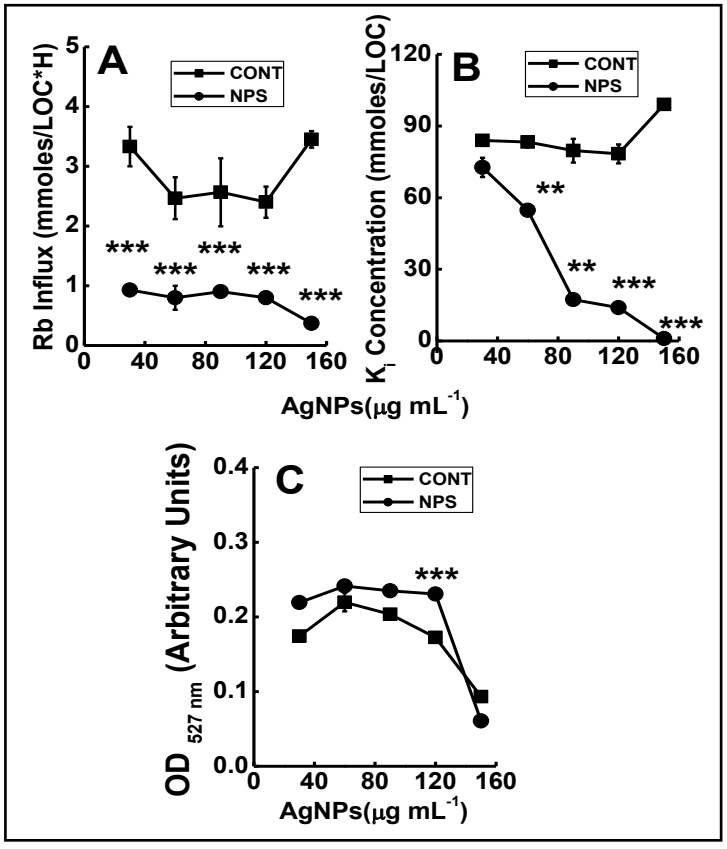

Fig. 7. Dose-response of Rb^+ influx, $[K]_i$, and Hb_c ODs in CR AgNPs-treated RBCs from human cord blood. Cord blood obtained at MVH was subjected to the procedures described in Materials and Methods and Fig. 1. During the flux period, RBCs for the CONT and NPS conditions were incubated with AgNPs at the following concentrations: 30, 60, 90, 120 and 150 μgmL^{-1}, at 37 °C for 60 min. In the control, identical volume of water instead of AgNPs was added for each concentration of AgNPs while maintaining constant osmolality along the concentration range. See legend to Fig. 3. for further details. Rb^+ influx, $[K]_i$ and Hb_c ODs were determined as described in Materials and Methods. Values are means ± S.D. Paired t-test was used to determine the statistical difference between NPS vs CONT. A) ***$p<0.0001$, n = 3 for Rb^+ influx, B) ***$p<0.0001$, n = 3 and **$p<0.001$, n = 3) for $[K]_i$ concentration, and C) ***$p <0.0001$, n = 3 for Hb_c ODs.

The degree of hemolysis, i.e., Hb_c ODs, as a function of AgNPs concentration, was determined in the samples already used for Fig. 7A and 7B (Fig. 7C). While the NPS ODs were relatively constant between 30–120 μg mL^{-1}, the CONT ODs showed a decreasing linear relationship at concentrations of 60 μg mL^{-1} and higher, and at 120 μg mL^{-1} there was a statistically significant difference between CONT and NPS. Because the Hb_c ODs of CONTC were the highest of the three conditions tested (Results not shown), the lower ODs in CONT and NSP are indicative of higher hemolysis or more swelling or both with the sequence CONT > NPS (Fig. 7C). At higher AgNPs concentration, both RBCs in the CONT and NPS conditions hemolyzed. Because the AgNPs were suspended in water, increasing the AgNPs concentrations would cause a decrease in the osmolality. To avoid a volume effect instead of an effect of the NPs, the osmolality was maintained constant along the concentration range tested.

In conclusion, CR AgNPs inhibited Rb^+ influx and depleted RBCs of K^+ in a time- and dose-dependent manner through a mechanism that needs further elucidation. Moreover, these results indicate that indeed CR-functionalized AgNPs are toxic to human RBCs.

Effect of cold storage on RBCs and interindividual variability

Fig. 2-8 indicate that CR AgNPs$^-$ cause significant changes in RBCs ion transport properties and in a time- and dose-dependent manner. These changes have different origins and demonstrated interindividual variability. A summary of these experiments is shown in Fig. 8A and B where the Rb^+ influx and $[K]_i$, respectively, were measured in fresh or stored adult and cord blood, under the different experimental conditions described above (Fig. 3, 5, and 7-8, i.e., CONTC, CONT and NPS). The most striking finding was that CR AgNPs$^-$ consistently inhibited Rb^+ influx and depleted the cells of K^+, independently of the blood source and time of storage in the cold. In some of the samples where RBCs were kept longer at 4 °C, the change in Rb^+ influx and $[K]_i$ was variable and appeared to be more pronounced for Rb^+ than for K^+ (compare Fig. 8A and B). Hence CR AgNPs are highly toxic under the conditions tested in eight donors.

Functionalization has been shown to be an important feature of AgNPs that may significantly affect their toxicity and could render them amenable for diagnostic and therapeutic purposes [4-6, 49, 69-72]. Questions such as: Are all AgNPs as toxic as the CR NPs or do differentially functionalized AgNPs vary in their toxicity to ion transport in HRBCs? To this end, the effect of LM-functionalized AgNPs$^-$ was studied on RBC ion transport. These AgNPs, have citrate groups on the surface, in contrast to CR AgNPs functionalized with borate.

Effect of LM AgNPs on Rb^+ influx, $[K]_i$, and Hb_c ODs in cord RBCs

In a parallel experiment with CR AgNPs$^-$ that inhibited ion movements by ~90% at 150 μg mL^{-1} (data not shown, see similar results in Fig. 3), Lee-Meisel AgNPs inhibited Rb^+ influx by about 50 % (Fig. 9A) and K^+ loss only by ~ 20 % (Fig. 9B), whereas there were no changes between the CONT and CONTC conditions (Fig. 9A & B). In addition, the Hb_c ODs were practically unchanged in CONTC, CONT and NPS (Fig. 9C), indicating that no apparent hemolysis occurred by exposure of HRBCs to LM AgNPs. These results indicate that AgNPs functionalized with citrate are less toxic to RBCs K^+ metabolism.

Time course of Rb^+ uptake, $[K]_i$, and Hb_c ODs as a function of LM AgNPs-exposure in cord RBCs

Like the kinetic studies with CR AgNPs, the effect of LM AgNPs on Rb^+ uptake, $[K]_i$ and Hb_c ODs was studied in RBCs from cord blood at 15, 30, and 60 min in the CONT and NPS conditions (Fig. 10). Rb^+ uptake in the control (CONT) was not a linear function of time, but rather increased by 2-fold between 15 and 60 min tending to saturate at the longer incubation times probably due to back-flux or to more than one mechanism of Rb^+ uptake. Furthermore,

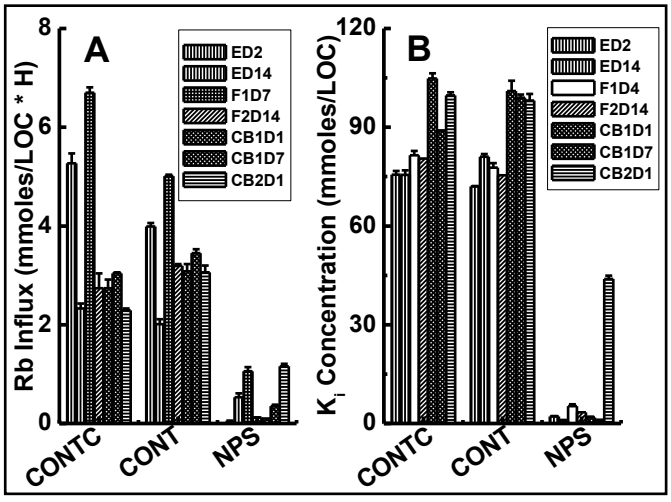

Fig. 8. Effect of storage and CR AgNPs on HRBCs, Rb^+ influx, and $[K]_i$ from different donors. RBCs obtained from adult donors at DCBC or cord blood from MVH were subjected to the procedures described in Materials and Methods. During the flux period, cells were incubated at 37 °C for 60 min under the conditions described in the legend to Fig. 3. Rb^+ influx and $[K]_i$ were determined as described in Materials and Methods. Values are means± S.D. Details are discussed in the text. E, F, CB represent RBCs from expired or fresh adult donors, and cord blood, respectively, whereas D represents days in storage at 4 °C. Each bar corresponds to different patients for CONTC, CONT, and NPS.

LM AgNPs (NPS) inhibited Rb^+ uptake from 30 % ($p < 0.05$) to 100 % ($p < 0.0001$) between 15 and 60 min vs. the control (Fig. 10A). In contrast, $[K]_i$ remained almost constant with time in both CONT and NPS, and the K^+ loss, although statistically significant ($p < 0.0005$) was only 10 % of the $[K]_i$ in the control (Fig. 10B). Notably, LM functionalized AgNPs had no effect on Hb_c ODs as a function of time between CONT and NPs (Fig. 10C). The decrease in Rb^+ uptake caused by the LM AgNPs was comparable to that induced by CR AgNPs (Fig. 6), whereas the decrease in $[K]_i$ was about 3-fold less than with the latter (compare Fig. 6 and 10). These results clearly indicate that LM AgNPs are less toxic to cord RBCs than CR AgNPs under similar experimental conditions.

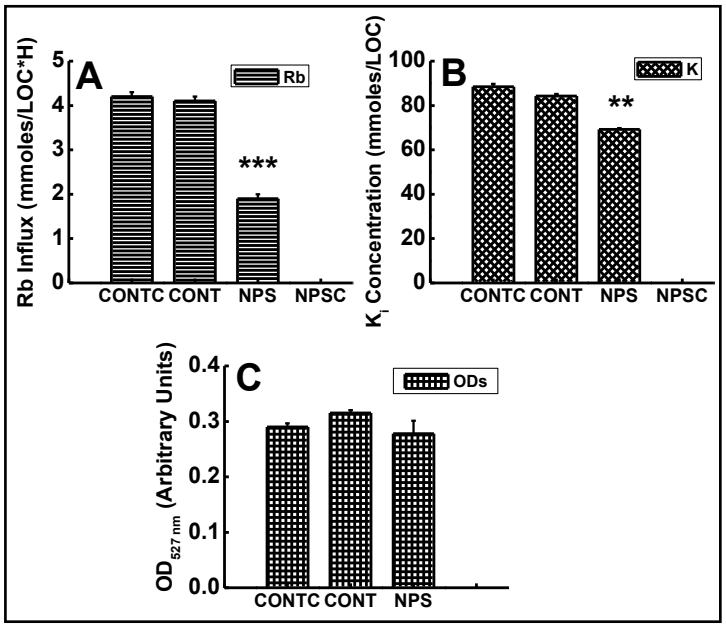

Fig. 9. Effect of LM AgNPs on Rb^+ influx, $[K]_i$, and Hb_c ODs for fresh cord RBCs. RBCs obtained from MVH were subjected to the different procedures described in Materials and Methods as shown in Fig. 1. During the flux period, cells were incubated at 37 °C for 60 min under the conditions described in legend to Fig. 3. Rb^+ influx, $[K]_i$ and Hb_c ODs were determined as described in Materials and Methods. Values are means ± S.D, n = 6 individual determinations for all the conditions tested. The statistical significance of the differences between NPS vs CONT, and CONT vs CONTC was determined by paired t- test. A) ***$p<0.0001$, n = 3 for Rb^+ influx, B) **$p<0.001$, n = 3 for $[K]_i$, and C) $p > 0.05$, n = 3 for Hb_c ODs.

So far, the effect of two types of functionalized AgNPs, CR and LM, was studied under different conditions and in different types of human blood, i.e., adult, either expired or fresh, and cord blood. These studies indicate that, independently of the type of blood and storage conditions, CR but not LM AgNPs caused depletion of RBC $[K]_i$. Further characterization of the mechanisms by which CR AgNPs alter ion transport involved studies on the effect of temperature (4 °C and 37 °C) on Rb^+ influx and $[K]_i$ in AgNPs-treated RBCs from human cord blood (Results not shown). Data indicate that AgNPs alter Rb^+ influx and $[K]_i$ through temperature-dependent pathways for both control (CONT) and experimental condition (NPS) and this effect was proportionally larger for Rb^+ influx than for K^+ loss. In addition, at 4 ºC, about 50 % of the Rb^+ influx and 60 % of K^+ loss was temperature-independent in NPS-treated RBCs when compared to their controls, suggesting ion movements through mechanisms that do not require metabolic energy.

To develop standards of AgNPs toxicity, an important question is whether there is interindividual variability for the effect of the $AgNPs^-$ tested in this study, and of AgNPs in general. Indeed, as it is shown for human cord RBCs from a different patient, the effect of CR $AgNPs^-$ on K^+ metabolism was less pronounced at 60 min in Fig. 6 than in Fig. 5 with only 60 % inhibition of Rb^+ influx and $[K]_i$ vs. the control. Furthermore, Fig. 8 clearly shows interindividual variability for a sample of N = 8 patients, albeit CR AgNPs were toxic for RBCs from the patients studied. These are important findings indicating that some individuals may be more susceptible than others to the effect of AgNPs, thus making the task of establishing safe and acceptable limits for the use of AgNPs for either diagnostic or therapeutic purposes, more complex.

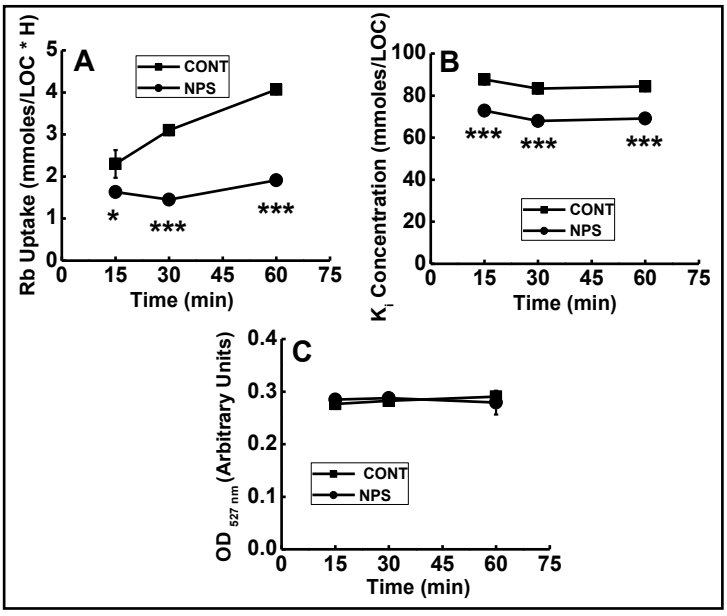

Fig. 10. Time course of Rb^+ uptake, $[K]_i$, and Hb_c ODs in LM AgNPs-treated RBCs from fresh human cord blood. RBCs were incubated at 37 °C for 15, 30, and 60 min. RBCs were obtained from MVH and subject to the different procedures described in Materials and Methods. A) Rb^+ influx, B) $[K]_i$, and C) Hb_c ODs were determined as described in Materials and Methods and conditions are as described in the legend to Fig. 3. Values are means ± S.D, n =3-6. The statistical significance of the difference between NPS vs CONT at the different time points was determined by either paired t- test or two sample t-test. A) ***p<0.0001, * p<0.05, B) *** p<0.0005, and C) p > 0.05.

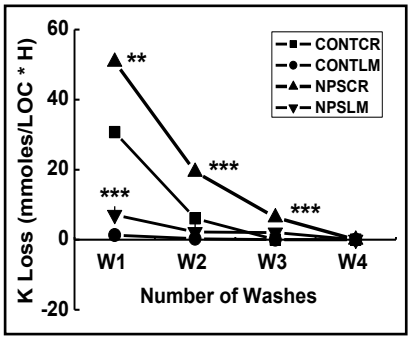

Fig. 11. Effect of AgNPs on K^+ loss in human cord blood. The figure represents K^+ in supernatants collected from each of the four washes done for CONT and NPs (see Fig. 3. for further details) from RBCs exposed to CR and LM AgNPs and plotted as a function of wash number. K^+ was released into the supernatant as a function of wash number according to the following sequence: NPSCR > CONTCR > NPSLM > CONTLM. Values are means ± S.D, n = 3-6. The statistical significance of the difference between NPSCR vs CONTCR and NPSLM vs CONTLM for W1, NPSCR vs CONTCR for W2 and W3 was determined by either paired t- test or two- sample t-test. ** p<0.05; *** p<0.00001.

K^+ concentration in supernatant, $[K]_o$, after washing RBCs treated with CR or LM AgNPs

To assess whether K^+ was lost from the cells into the media or remained adsorbed on the AgNPs surface after incubation in their presence, $[K]_o$ was determined in the supernatant fraction as a measure of the K^+ loss from RBCs. The K^+ loss from cells exposed to CR and LM AgNPs, decreased with increasing the number of washes, was higher in cells treated with CR than with LM AgNPs and followed the sequence NPSCR > CONTCR > NPSLM > CONTLM (Fig. 11). Furthermore, K^+ loss induced by either CR or LM AgNPs could be accounted for by appearance of K^+ in the extracellular space during the flux procedure as reflected by a rise in $[K]_o$ of the supernatants that were simultaneously collected after each wash. In other words, the difference in $[K]_i$ after 60 min exposure to NPs was equal to the total K^+ loss determined in the supernatants (data not shown), indicating that K^+ was not adsorbed on the NPs but it was released into the media. These results also support our findings (Fig. 3, 5, 7, 8, 9B, 10 and 11) of a higher toxicity of CR than LM NPs and demonstrate the important role of AgNPs functionalization for their biological effect.

Discussion

Nano-size particles cause more RBC hemolysis than larger particles due to their greater surface area which facilitates a larger release of Ag^+ from AgNPs by their direct interaction with the RBCs. In fact, released Ag^+ ions have been shown to be responsible for the AgNPs toxicity [40]. Small nano-size particles are more likely to be internalized into cell lines than the large ones [32, 33]. In various cell lines and animal models, different types of NPs are known to induce cytotoxicity. AgNPs are the most toxic NPs because of their metallic silver and high biological reactivity [34, 35]. Positively charged NPs are more toxic than the negatively charged [46], because the RBC surface charge is negative and thus possess higher affinity for the positively charged NPs. In human RBCs, QDs coated with D-penicillamine, a zwitterionic amino acid ligand (D-penicillamine DPA-QDs), enter the cells by a passive transport mechanism and their toxicity depends, in general, on their size (the smaller the more toxic) and charge (cationic QDs interacting stronger with cells than anionic counterparts) [32]. However, despite some cautious generalizations [32], numerous factors contribute to NPs toxicity, which depends on both the NPs physicochemical properties and the biological material with which they interact [46]. This is the case in the present study, where negatively charged AgNPs were expected to be less bioavailable and toxic than positive ones, as it was found in Vero 76 cells [53]. In contrast to expectations, $AgNPs^-$ induced complete $[K]_i$ depletion in HRBCs from all but one of the donors tested (Fig. 3B, 5B, 7B, and 8B), and this was independent of the type of cells, adult or cord, fresh or expired and of the time in cold storage (Fig. 3B, 5B, 7B, and 8B), but strongly dependent on the functionalization of the NPs. In fact, this study shows that CR AgNPs were more toxic than the LM (Fig. 3B, 5B, 7B- 8B and 11 vs. Fig. 9-11), and this is supported by the lower Hb_c ODs in CONT and NSP in Figure7C, which are indicative of higher hemolysis with the sequence CONT > NPS. Furthermore, LM AgNPs did not lyse RBCs (Fig. 10C) despite that the AgNPs-treated RBCs should have decreased their volume due to the inhibition of Rb^+ uptake (Fig. 10A) and the increase in K^+_i loss (Fig. 10B), once more pointing to a less toxic effect of the latter when compared to CR AgNPs.

Furthermore, few studies providing a detailed mechanism of AgNPs toxicity are available, despite the abundant applications of AgNPs in industry and in AgNPs-based medicine where they have been introduced into human tissue upon administration by either injection or through skin exposure. These penetration routes will likely lead to interaction of AgNPs with blood tissue and its components [47, 48]. These interactions can be either beneficial or detrimental. For instance, AgNPs help to activate synergistically immune responses by human monocytes [49]. In contrast, AgNPs cause structural damage of erythrocytes and change erythrocyte rheology [38]. AgNPs also cause platelet aggregation and hemolysis of RBCs [50, 51].

Likewise, despite a large body of information described above, the mechanisms involving toxicity to RBCs remain to be elucidated [51]. To fill this gap, this study focused on the effect of AgNPs on RBC cellular ionic homeostasis and used differentially functionalized silver nanoparticles as experimental materials to treat RBCs. To achieve this goal, RBC Rb^+ influx, $[K]_i$, and Hb_c ODs were determined in HRBCs under different experimental conditions, and as a function of NPs length of exposure, concentrations and functionalization.

Different types of human RBCs were used in the present study (adult or cord blood, expired or fresh, or stored refrigerated for different periods of time, from 0 to 14 days), and treated with two types of negatively charged functionalized AgNPs of an average diameter of 10 nm, Creighton and Lee Meisel. CR AgNPs inhibited Rb^+ influx by 50% to 80 % (Fig. 3A, and 5A-7A) and depleted the cells of $[K]_i$ by 50 to 90 % (Fig. 3B and 5B-7B). LM AgNPs inhibited Rb influx by 50 % and depleted $[K]_i$ by an average of 15 % (Fig. 9 and 10), in contrast to CR AgNPs. Our results show inter-individual variability for $[K]_i$ in expired, fresh, or stored RBCs. However, it was not clear from the transport data whether adsorbed NPs on the RBC surface were responsible for both K^+ loss and inhibition of Rb^+ entry in the cells. In contrast to this argument, Fig. 4 shows that AgNPs exerted their effect by internalization of the NPs in

the RBCs. This finding is further supported by studies on internalization of D-penicillamine (DPA)-QD in human RBCs [40]. The K^+ loss observed upon cold storage (Fig. 8B) is further supported by findings of K^+ loss when blood is maintained under refrigeration [73].

In summary, CR AgNPs inhibited Rb^+ influx and K^+_i loss in a time- and dose-dependent manner (Fig. 6 and 7). LM AgNPs also altered RBC permeability to Rb^+ and K^+ in a time-dependent manner (Fig. 10). The K^+ loss induced by either CR or LM AgNPs could be accounted for by appearance of K^+ in the extracellular space during the flux procedure as reflected in $[K]_o$ collected after each wash (Fig. 11).

Based on the results described above, the present study shows that both CR and LM AgNPs altered K^+ homeostasis in human RBCs. During these studies, however, it remained to be determined whether this effect was due to extracellular or internalized AgNPs in HRBCs. By using CytoViva® hyperspectral imaging, AgNPs were found to be internalized in human RBCs (Fig. 4 B-D), and thus their effect may have been due to their internalization (Fig. 4). Our findings in human RBCs agree with reports in human and nucleated fish RBCs where zwitterionic quantum dots and AgNPs toxicity is caused by internalization of the NPs [32, 33, 44].

Conclusion

CR and LM functionalized AgNPs were found to alter the K^+ levels in RBCs in a time- and dose-dependent manner, and this effect appeared to be induced by AgNPs internalization, which led to a massive intracellular K^+ loss that could be accounted for by its presence in the RBCs extracellular compartment. This is indeed an important finding indicative of potential and serious complications during AgNPs *in vivo* administration to patients receiving complex drug treatments that could enhance the NPs effect/s, and especially in patients suffering from cardiovascular diseases and kidney insufficiency for whom sudden changes in plasma K^+ could lead to life threatening situations. Of equal importance, our findings show that alterations of membrane permeability and, consequently, ion transport are one of the early events leading to cell death (or hemolysis for RBCs), thus becoming a strategic point for applying maneuvers to reverse it.

Acknowledgements

Author Contributions: N.C.A. and P.K.L. conception and design of research; P.K.A. performed the experiments with initial help from N.C.A., P.K.A., N.C.A., and P.K.L., analyzed data; N.C.A., P.K.L. and P.K.A. interpreted results of experiments; P.K.A., and N.C.A. prepared figures; N.C.A. drafted manuscript; N.C.A., P.K.L. and P.K.A. edited and revised manuscript; N.C.A and P.K.L approved final version of manuscript. I.E.P-S and A.S.L.P. synthesized the AgNPs, provided important scientific and experimental input related to nanotechnology and the manuscript, and facilitated procurement of blood from the Dayton Community Blood Center. J.L.Y. procured cord blood from his patients at the Miami Valley Hospital, facilitated writing, submission, and approval of Informed Consent Forms, IRBs and IBCs, and participated in critical discussions about the clinical implications of the study.

Images and data illustrated in Fig. 4 were provided compliments of CytoViva®, Inc. www.cytoviva.com, info@cytoviva.com, 570 Devall Drive Suite 301, Auburn, AL 36832. Human adult blood was kindly provided by the Dayton Community Blood Center, and human cord blood by the Miami Valley Hospital, Dayton, OH. Dr. Marjorie Markopoulos participated in the initial stages of this study. Drs. Marjorie Markopoulos and Rose Maxwell facilitated the approval of IRBs, IBCs, amendments, and compliance with administrative regulations at Wright State University and MVH, respectively.

Funding Sources: This work was supported, in part, by the National Science Foundation (Awards # 1438340 and 1726095), Department of Pharmacology and Toxicology, Department of Chemistry, and Wright State Foundation.

Disclosure Statement

The authors report no conflict of interest.

References

1 Roco MC, Mirkin CA, Hersam MC: Nanotechnology research directions for societal needs in 2020: summary of international study. J Nanopart Res 2011;13:897-919.
2 Salisbury RL, Agans R, Huddleston ME, Snyder A, Mendlein A, Hussain S: Chapter 21 - Toxicological Mechanisms of Engineered Nanomaterials: Role of Material Properties in Inducing Different Biological Responses; in: Slikker W, Paule MG, and Wang C, (eds): Handbook of Developmental Neurotoxicology (Second Edition). Academic Press, 2018, pp 237-249.
3 Zhang XD, Jing Y, Song S, Yang J, Wang JY, Xue X, Min Y, Park G, Shen X, Sun YM, Jeong U: Catalytic topological insulator Bi2Se3 nanoparticles for *in vivo* protection against ionizing radiation. Nanomedicine 2017;13:1597-1605.
4 Chaloupka K, Malam Y, Seifalian AM: Nanosilver as a new generation of nanoproduct in biomedical applications. Trends Biotechnol 2010;28:580-588.
5 Pal S, Tak YK, Song JM: Does the Antibacterial Activity of Silver Nanoparticles Depend on the Shape of the Nanoparticle? A Study of the Gram-Negative Bacterium Escherichia coli. Appl Environ Microbiol 2007;73:1712-1720.
6 Wijnhoven SWP, Peijnenburg WJGM, Herberts CA, Hagens WI, Oomen AG, Heugens EHW, Roszek B, Bisschops J, Gosens I, Van De Meent D, Dekkers S, De Jong WH, van Zijverden M, Sips AJAM, Geertsma RE: Nano-silver - A review of available data and knowledge gaps in human and environmental risk assessment. Nanotoxicology 2009;3:109.
7 Morones JR, Elechiguerra JL, Camacho A, Holt K, Kouri JB, Tapia Ramírez J, Yacaman MJ: The bactericidal effect of silver nanoparticles. Nanotechnology 2005;16:2346.
8 Rai M, Yadav A, Gade A: Silver nanoparticles as a new generation of antimicrobials. Biotechnol Adv 2009;27:76-83.
9 Rai MK, Deshmukh SD, Ingle AP, Gade AK: Silver nanoparticles: the powerful nanoweapon against multidrug-resistant bacteria. J Appl Microbiol 2012;112:841-852.
10 Arafat HH, El-Sayed MH, Askora A: Silver Nanoweapons: A novel Tool against Multidrug Resistant Bacteria. Biosci Biotech Res Asia 2016;13:95-101.
11 Naqvi SZH, Kiran U, Ali MI, Jamal A, Hameed A, Ahmed S, Ali N: Combined efficacy of biologically synthesized silver nanoparticles and different antibiotics against multidrug-resistant bacteria. Int J Nanomedicine 2013;8:3187-3195.
12 Rogers JV, Parkinson CV, Choi YW, Speshock JL, Hussain SM: A Preliminary Assessment of Silver Nanoparticle Inhibition of Monkeypox Virus Plaque Formation. Nanoscale Res Lett 2008;3:129.
13 Shubayev VI, Pisanic TR, Jin S: Magnetic nanoparticles for theragnostics. Adv Drug Deliv Rev 2009;61:467-477.
14 Wan G, Ruan L, Yin Y, Yang T, Ge M, Cheng X: Effects of silver nanoparticles in combination with antibiotics on the resistant bacteria Acinetobacter baumannii. Int J Nanomedicine 2016;11:3789-3800.
15 Braydich-Stolle L, Hussain S, Schlager JJ, Hofmann MC: *In vitro* cytotoxicity of nanoparticles in mammalian germline stem cells. Toxicol Sci 2005;88:412-419.
16 Ahamed M, Karns M, Goodson M, Rowe J, Hussain SM, Schlager JJ, Hong Y: DNA damage response to different surface chemistry of silver nanoparticles in mammalian cells. Toxicol Appl Pharmacol 2008;233:404-410.

17 Braydich-Stolle LK, Lucas B, Schrand A, Murdock RC, Lee T, Schlager JJ, Hussain SM, Hofmann MC: Silver nanoparticles disrupt GDNF/Fyn kinase signaling in spermatogonial stem cells. Toxicol Sci 2010;116:577-589.
18 Atiyeh BS, Costagliola M, Hayek SN, Dibo SA: Effect of silver on burn wound infection control and healing: Review of the literature. Burns 2007;33:139-148.
19 Carlson C, Hussain SM, Schrand AM, Braydich-Stolle LK, Hess KL, Jones RL, Schlager JJ: Unique cellular interaction of silver nanoparticles: size-dependent generation of reactive oxygen species. J Phys Chem B 2008;112:13608-13619.
20 Kim S, Choi JE, Choi J, Chung KH, Park K, Yi J, Ryu DY: Oxidative stress-dependent toxicity of silver nanoparticles in human hepatoma cells. Toxicol In Vitro 2009;23:1076-1084.
21 Beer C, Foldbjerg R, Hayashi Y, Sutherland DS, Autrup H: Toxicity of silver nanoparticles—Nanoparticle or silver ion? Toxicol Lett 2012;208:286-292.
22 Foldbjerg R, Dang DA, Autrup H: Cytotoxicity and genotoxicity of silver nanoparticles in the human lung cancer cell line, A549. Arch Toxicol 2011;85:743-750.
23 Lam PK, Chan ESY, Ho WS, Liew CT: *In vitro* cytotoxicity testing of a nanocrystalline silver dressing (Acticoat) on cultured keratinocytes. Br J Biomed Sci 2004;61:125-127.
24 Fong J, Wood F: Nanocrystalline silver dressings in wound management: a review. Int J Nanomedicine 2006;1:441-449.
25 Ahamed M, Posgai R, Gorey TJ, Nielsen M, Hussain SM, Rowe JJ: Silver nanoparticles induced heat shock protein 70, oxidative stress and apoptosis in Drosophila melanogaster. Toxicol Appl Pharmacol 2010;242:263-269.
26 Hussain SM, Braydich-Stolle LK, Schrand AM, Murdock RC, Yu KO, Mattie DM, Schlager JJ, Terrones M: Toxicity Evaluation for Safe Use of Nanomaterials: Recent Achievements and Technical Challenges. Adv Mater 2009;21:1549-1559.
27 Hussain SM, Hess KL, Gearhart JM, Geiss KT, Schlager JJ: *In vitro* toxicity of nanoparticles in BRL 3A rat liver cells. Toxicol In Vitro 2005;19:975-983.
28 Schrand AM, Rahman MF, Hussain SM, Schlager JJ, Smith DA, Syed AF: Metal-based nanoparticles and their toxicity assessment. Wiley Interdiscip Rev Nanomed Nanobiotechnol 2010;2:544-568.
29 Stensberg MC, Wei Q, McLamore ES, Porterfield DM, Wei A, Sepúlveda MS: Toxicological studies on silver nanoparticles: challenges and opportunities in assessment, monitoring and imaging. Nanomedicine (Lond) 2011;6:879-898.
30 Teodoro JS, Simões AM, Duarte FV, Rolo AP, Murdoch RC, Hussain SM, Palmeira CM: Assessment of the toxicity of silver nanoparticles *in vitro*: A mitochondrial perspective. Toxicology In Vitro 2011;25:664-670.
31 Trickler WJ, Lantz SM, Murdock RC, Schrand AM, Robinson BL, Newport GD, Schlager JJ, Oldenburg SJ, Paule MG, Slikker JW, Hussain SM, Ali SF: Silver Nanoparticle Induced Blood-Brain Barrier Inflammation and Increased Permeability in Primary Rat Brain Microvessel Endothelial Cells. Toxicol Sci 2010;118:160-170.
32 Shang L, Nienhaus K, Nienhaus GU: Engineered nanoparticles interacting with cells: size matters. J Nanobiotechnology 2014;12:5.
33 Wang T, Bai J, Jiang X, Nienhaus GU: Cellular uptake of nanoparticles by membrane penetration: a study combining confocal microscopy with FTIR spectroelectrochemistry. ACS Nano 2012;6:1251-1259.
34 AshaRani P, Hande MP, Valiyaveettil S: Anti-proliferative activity of silver nanoparticles. BMC Cell Biol 2009;10:65.
35 AshaRani PV, Low Kah Mun G, Hande MP, Valiyaveettil S: Cytotoxicity and Genotoxicity of Silver Nanoparticles in Human Cells. ACS Nano 2009;3:279-290.
36 Comfort KK, Braydich-Stolle LK, Maurer EI, Hussain SM: Less Is More: Long-Term *in vitro* Exposure to Low Levels of Silver Nanoparticles Provides New Insights for Nanomaterial Evaluation. ACS Nano 2014;8:3260-3271.
37 Marshall JP, Ii, Schneider RP: Systemic argyria secondary to topical silver nitrate. Arch Dermatol 1977;113:1077-1079.
38 Asharani PV, Sethu S, Vadukumpully S, Zhong S, Lim CT, Hande MP, Valiyaveettil S: Investigations on the Structural Damage in Human Erythrocytes Exposed to Silver, Gold, and Platinum Nanoparticles. Adv Funct Mater 2010;20:1233-1242.

39 McShan D, Ray PC, Yu H: Molecular Toxicity Mechanism of Nanosilver. J Food Drug Anal 2014;22:116-127.
40 Choi J, Reipa V, Hitchins VM, Goering PL, Malinauskas RA: Physicochemical characterization and *in vitro* hemolysis evaluation of silver nanoparticles. Toxicol Sci 2011;123:133-143.
41 Maurer EI, Sharma M, Schlager JJ, Hussain SM: Systematic analysis of silver nanoparticle ionic dissolution by tangential flow filtration: toxicological implications. Nanotoxicology 2014;8:718-727.
42 van Aerle R, Lange A, Moorhouse A, Paszkiewicz K, Ball K, Johnston BD, de-Bastos E, Booth T, Tyler CR, Santos EM: Molecular Mechanisms of Toxicity of Silver Nanoparticles in Zebrafish Embryos. Environ Sci Technol 2013;47:8005-8014.
43 Bankapur A, Barkur S, Chidangil S, Mathur D: A Micro-Raman Study of Live, Single Red Blood Cells (RBCs) Treated with AgNO3 Nanoparticles. Plos One 2014;9:e103493.
44 Chen LQ, Fang L, Ling J, Ding CZ, Kang B, Huang CZ: Nanotoxicity of Silver Nanoparticles to Red Blood Cells: Size Dependent Adsorption, Uptake, and Hemolytic Activity. Chem Res Toxicol 2015;28:501-509.
45 Składanowski M, Golinska P, Rudnicka K, Dahm H, Rai M: Evaluation of cytotoxicity, immune compatibility and antibacterial activity of biogenic silver nanoparticles. Med Microbiol Immunol 2016;205:603-613.
46 Shin SW, Song IH, Um SH: Role of physicochemical properties in nanoparticle toxicity. Nanomaterials (Basel) 2015;5:1351-1365.
47 Quadros ME, Marr LC: Environmental and human health risks of aerosolized silver nanoparticles. J Air Waste Manag Assoc 2010;60:770-781.
48 Yah CS, Simate GS, Iyuke SE: Nanoparticles toxicity and their routes of exposures. Pak J Pharm Sci 2012;25:477-491.
49 Yang EJ, Kim S, Kim JS, Choi IH: Inflammasome formation and IL-1β release by human blood monocytes in response to silver nanoparticles. Biomaterials 2012;33:6858-6867.
50 Huang H, Lai W, Cui M, Liang L, Lin Y, Fang Q, Liu Y, Xie L: An Evaluation of Blood Compatibility of Silver Nanoparticles. Sci Rep 2016;6:25518.
51 Laloy J, Minet V, Alpan L, Mullier F, Beken S, Toussaint O, Lucas S, Dogné JM: Impact of silver nanoparticles on haemolysis, platelet function and coagulation. Nanobiomedicine (Rij) 2014;1:4.
52 Fabrega J, Luoma SN, Tyler CR, Galloway TS, Lead JR: Silver nanoparticles: Behaviour and effects in the aquatic environment. Environ Int 2011;37:517-531.
53 Paluri SLA, Ryan JD, Lam NH, Nepal D, Sizemore IE: Analytical-Based Methodologies for Examining the *In vitro* Absorption, Distribution, Metabolism, and Elimination (ADME) of Silver Nanoparticles. Small 2017;13:1603093.
54 Alla PK, Lauf PK, Pavel I, Paluri A, Markopoulos M, Yaklic J, Adragna NC: Internalized silver nanoparticles alter ion transport and hemoglobin spectrum in human red blood cells. FASEB J 2016;30:lb620.
55 Alla PK, Lauf PK, Sizmore IE, Paluri SLA, Yaklic J, Adragna NC: Not all silver nanoparticles are equal: Effect of functionalization on K homeostasis in human red blood cells. FASEB J 2017;31:lb685.
56 Trefry JC, Monahan JL, Weaver KM, Meyerhoefer AJ, Markopolous MM, Arnold ZS, Wooley DP, Pavel IE: Size Selection and Concentration of Silver Nanoparticles by Tangential Flow Ultrafiltration for SERS-Based Biosensors. J Am Chem Soc 2010;132:10970-10972.
57 Mulfinger L, Solomon SD, Bahadory M, Jeyarajasingam AV, Rutkowsky SA, Boritz C: Synthesis and Study of Silver Nanoparticles. J Chem Educ 2007;84:322.
58 Creighton JA, Blatchford CG, Albrecht MG: Plasma resonance enhancement of Raman scattering by pyridine adsorbed on silver or gold sol particles of size comparable to the excitation wavelengthJ Chem Soc Faraday Trans 2 1979;75:790-798.
59 Wan Y, Guo Z, Jiang X, Fang K, Lu X, Zhang Y, Gu N: Quasi-spherical silver nanoparticles: Aqueous synthesis and size control by the seed-mediated Lee–Meisel method. J Colloid Interface Sci 2013;394:263-268.
60 Anders CB, Baker JD, Stahler AC, Williams AJ, Sisco JN, Trefry JC, Wooley DP, Pavel Sizemore IE: Tangential flow ultrafiltration: a "green" method for the size selection and concentration of colloidal silver nanoparticles. J Vis Exp 2012; DOI:10.3791/41674167.
61 Dorney KM, Baker JD, Edwards ML, Kanel SR, O'Malley M, Pavel Sizemore IE: Tangential Flow Filtration of Colloidal Silver Nanoparticles: A "Green" Laboratory Experiment for Chemistry and Engineering Students. J Chem Educ 2014;91:1044-1049.
62 Paluri SL: Synthesis, Characterization and Manipulation of Creighton Silver Nanoparticles for Future Cytotoxicity Studies. Wright State University CORE Scholar, 2011, Paper 536.

63 D'Alessandro A, Hansen KC, Silliman CC, Moore EE, Kelher M, Banerjee A: Metabolomics of AS-5 RBC supernatants following routine storage. Vox Sang 2015;108:131-140.
64 D'Alessandro A, Liumbruno G, Grazzini G, Zolla L: Red blood cell storage: the story so far. Blood Transfus 2010;8:82-88.
65 van Kampen EJ, Zijlstra WG: Spectrophotometry of Hemoglobin and Hemoglobin Derivatives. Adv Clin Chem 1983;23:199-257.
66 Lauf PK, Adragna NC, Dupre N, Bouchard JP, Rouleau GA: K-Cl cotransport in red blood cells from patients with KCC3 isoform mutants. Biochem Cell Biol 2006;84:1034-1044.
67 Pauling L, Coryell CD: The Magnetic Properties and Structure of Hemoglobin, Oxyhemoglobin and Carbonmonoxyhemoglobin. Proc Natl Acad Sci U S A 1936;22:210-216.
68 Bian Y, Kim K, Ngo T, Kim I, Bae ON, Lim KM, Chung JH: Silver nanoparticles promote procoagulant activity of red blood cells: a potential risk of thrombosis in susceptible population. Part Fibre Toxicol 2019;16:9.
69 Nguyen KC, Seligy VL, Massarsky A, Moon TW, Rippstein P, Tan J, Tayabali AF: Comparison of toxicity of uncoated and coated silver nanoparticles. J Phys Conf Ser 2013;429:012025.
70 Wojnicki M, Luty-Błocho M, Kotańska M, Wytrwal M, Tokarski T, Krupa A, Kołaczkowski M, Bucki A, Kobielusz M: Novel and effective synthesis protocol of AgNPs functionalized using L-cysteine as a potential drug carrier. Naunyn Schmiedebergs Arch Pharmacol 2018;391:123-130.
71 Wu F, Harper B, Harper S: Differential dissolution and toxicity of surface functionalized silver nanoparticles in small-scale microcosms: impacts of community complexity. Environ Sci Nano 2017;4:359-372.
72 Zhang X-F, Shen W, Gurunathan S: Silver Nanoparticle-Mediated Cellular Responses in Various Cell Lines: An *in vitro* Model. Int J Mol Sci 2016;17:1603.
73 Hess JR, Greenwalt TG: Storage of red blood cells: New approaches. Transfus Med Rev 2002;16:283-295.